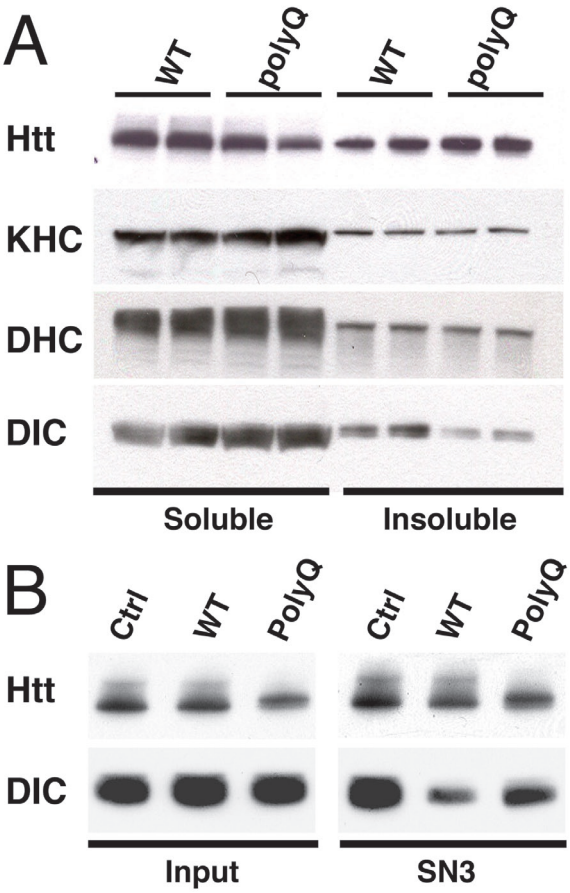


**Supplemental Figure 1. PolyQ-Htt does not affect motor protein solubility. A**) Brain lysates from wild type and $Hdh^{Q109}$ knock-in mice expressing endogenous levels of normal (WT-Htt) or pathogenic Htt (polyQ-Htt) were fractionated into detergent (TX-100) soluble and insoluble fractions. The distribution of major subunits of conventional kinesin and cytoplasmic dynein subunits were analyzed by immunoblot: Kin: (kinesin-1, kinesin heavy chain), DHC (dynein heavy chain); DIC: (dynein intermediate chain), Note that while Huntingtin (Htt) protein partitions similarly in both fractions, the bulk of molecular motors was recovered in the supernatant fraction. There was no evidence of increased motor protein insolubility induced by polyQ-Htt expression. **B**) Detergent-soluble brain lysates from wild type (WT-Htt) and $Hdh^{Q109}$ knock-in (polyQ-Htt) mice were subjected to three cycles of immunoprecipitation with antibodies against DIC, as in **Fig. 1B**. Aliquots of input material (Input) or the supernatant after three immunoprecipitation cycles (SN3) were analyzed by immunoblot with antibodies against DIC and Htt. Note the marked depletion of DIC immunoreactivity after immunoprecipitation with DIC-specific antibodies. Immunoprecipitates with a non-immune IgG (Ctrl) served as a control for non-specific precipitation of proteins in these experiments. In contrast, no change in Htt levels was detected, regardless of mouse genotype.

Nature Neuroscience: doi:10.1038/nn.2346

A

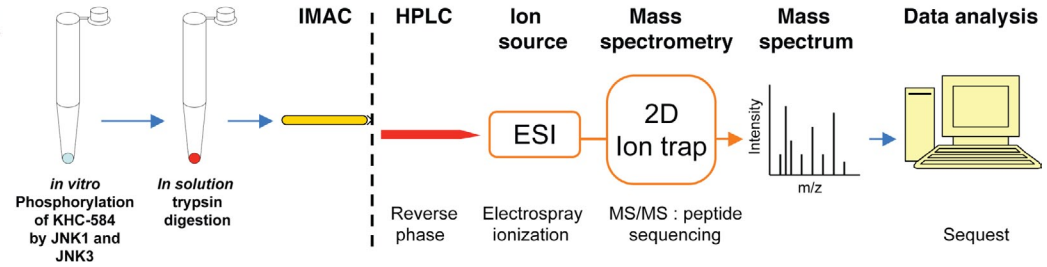


B

**KHC-584**

HHHHHHMADPAECSIKVMCRFRPLNEAEILRGDKFIRKFKGEETVVIGQGKPYVFDRVLPPNTTQEQVYNACA
KQIVKDVLEGYNGTIFAYGQTSSGKTHTMEGKLHDPQLMGIIPRIAHDIFDHIYSMDENLEFHIKVSYFEIYLDKI
RDLLDVSKTNLAVHEDKNRVPYVKGCTER**FVSS*PEEVMDVIDEGK**ANRHVAVTNMNEHSSRSHSIFLINIKQE
NVETEKKLSGKLYLVDLAGSEKVSKTGAEGAVLDEAKNINKSLSALGNVISALAEGTKTHVPYRDSKMTRILQD
SLGGNCRTTIVICCSPSVFNEAETKSTLMFGQRAKTIKNTVSVNLELTAEEWKKKYEKEKEKNKALKSVIQHLE
VELNRWRNGEAVPEDEQISAKDHKSLEPCDNTPIIDNITPVVDGISAEKEKYDEEITSLYRQLDDKDDEINQQS
QLAEKLKQQMLDQDELLASTRRDYEKIQEELTRLQIENEAAKDEVKEVLQALEELAVNYDQKSQEVEDKTRAN
EQLTDELAQKTTTLTTTQRELSQLQELSNHQKKRATEILNLLLKDLGEIGGIIGTNDVKTLADVNGVIEEEF

Protein coding for the first 584 aa of kinesin1-c from rat. Coverage of the 584 aa fragment is 72%

C

| Ion charge (a) | MH+ (ion mass) (b) | Xcorr (c) | dCn (d) | Sequence (e) |
|---|---|---|---|---|
| 2 | 1862.0 (-1.4) | 2.8069 | 0.395 | **R.FVSS*PEEVMDVIDEGK.A** |

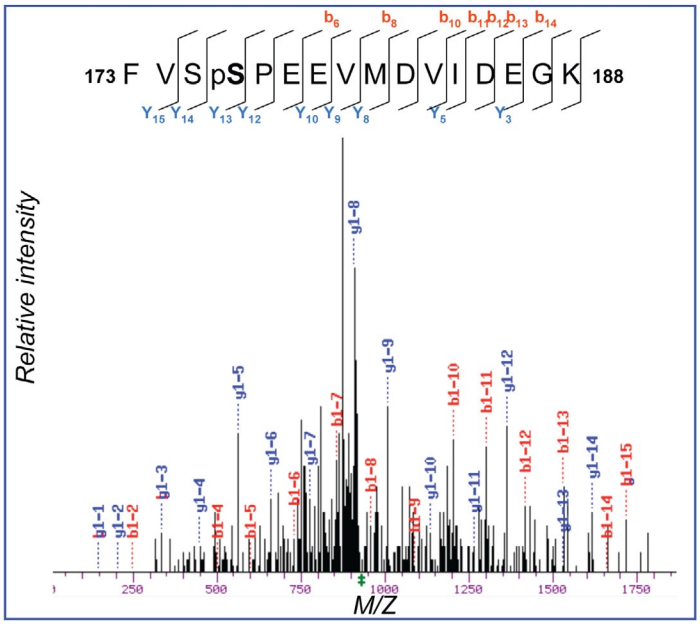


**Supplemental Figure 2. Mass spectrometry analysis of kinesin-1**. **A)** Diagram of mass spectrometry protocols for analysis of kinesin-1 phosphorylation by JNK3 and JNK1. **B)** The amino acid sequence of the $KHC^{584}$ construct is shown. Residues in red indicate amino acid coverage (72%). The sequence corresponding to the motor domain of kinesin-1c (KIF5C) is outlined. The major phosphopeptide identified in these studies (amino acids 173-188) is marked in bold. **C)** Relevant details of the 173-188 phosphopeptide identification are shown including its sequence (e), charge (a), mass (b), cross correlation (c), and delta correlation (d) values (top). Mass spectrum of the 173-188 phosphopeptide. The graph plots ion intensity vs. mass (M) ion charge (Z) ratio for *b*+ (red) and *y*+ (blue) ions. The peptide sequence (top) shows a detail of the identified residues.

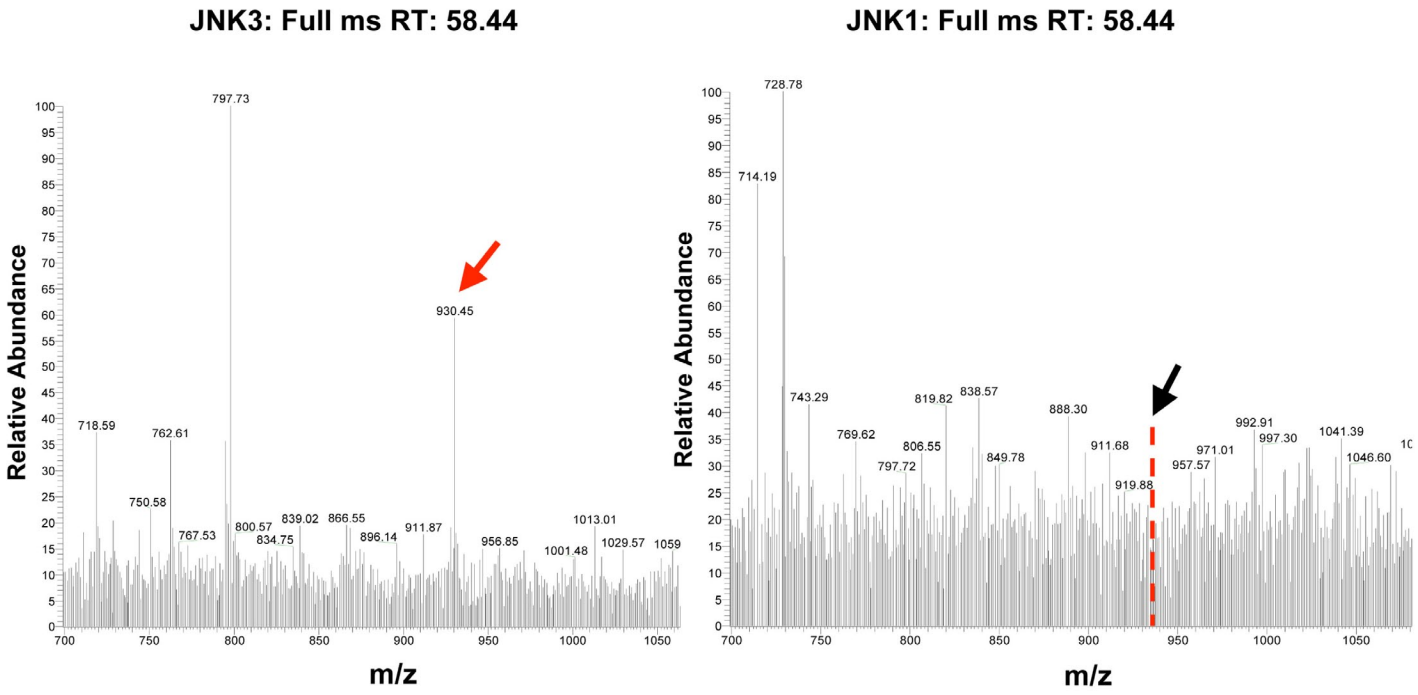


**Supplemental Figure 3. KHC$^{584}$ motor domain is phosphorylated by JNK3, but not by JNK1.** KHC$^{584}$ was phosphorylated *in vitro* using either JNK3 or JNK1 (as shown in **Figure 7B**), and samples processed for mass spectrometry analysis as described in Material and Methods. Full spectra (Full ms) corresponding to the retention time of the 173-188 phosphopeptide (RT: 58.44 minutes) are shown. The red arrow points the peak corresponding to the precursor ion of the phosphopeptide (m/z of 930.4). Note that this peak is present only in Full ms of JNK3-phosphorylated KHC$^{584}$ samples (left), but not in Full ms of JNK1-phosphorylated KHC$^{584}$ samples (right). The black arrow and dashed red line point the area of the Full ms where the peak for the precursor ion should be found. The activities of recombinant JNK1 and JNK3 were normalized using c-Jun as a substrate. These results indicate that JNK3, but not JNK1, can phosphorylate the Ser176 residue in kinesin-1.

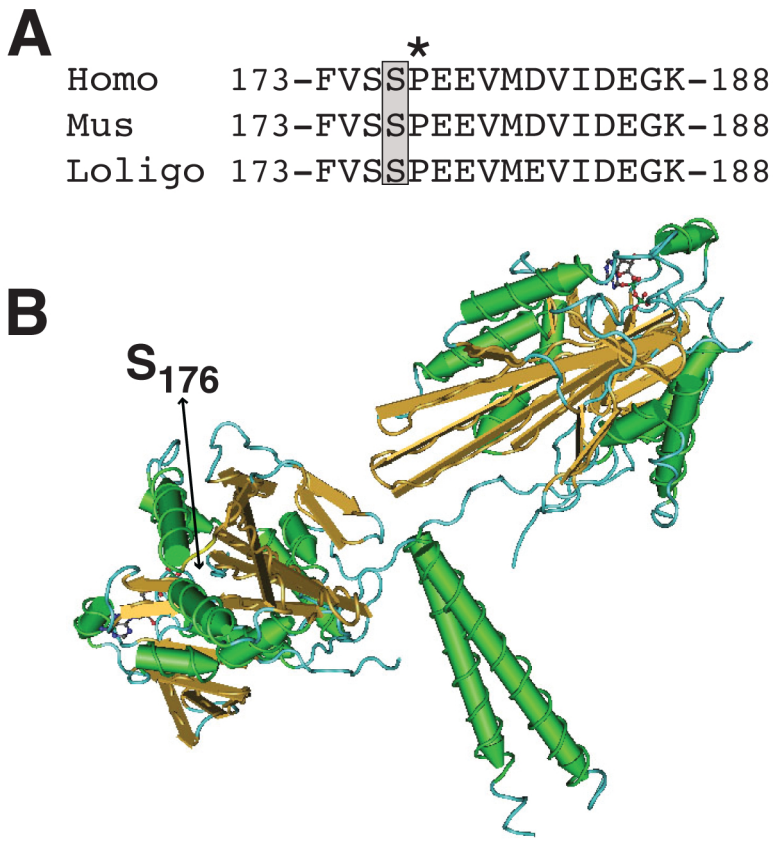


**Supplemental Figure 4. Ser176 is a conserved residue in the Kinesin-1 microtubule-binding domain. A)** Sequence alignment shows that Ser176 (boxed) is conserved among human, mouse and squid sequences for kinesin-1. **B)** Ser176 is located in a surface loop of KHC motor domain, a region implicated in binding of kinesin-1 to microtubules[36].

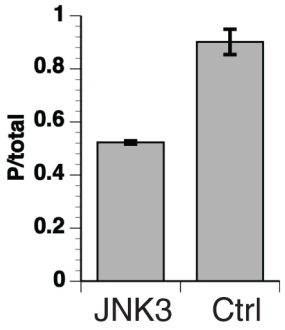


**Supplemental Figure 5. JNK3 phosphorylation of KHC$^{584}$ reduces binding to microtubules.** The histogram shows quantitation of immunoblots and autoradiograms in Figure 7B. The ratio of KHC$^{584}$ in microtubule pellets and supernatants (P/S) reveals a dramatic reduction in KHC binding to microtubules upon phosphorylation by JNK3.

Nature Neuroscience: doi:10.1038/nn.2346

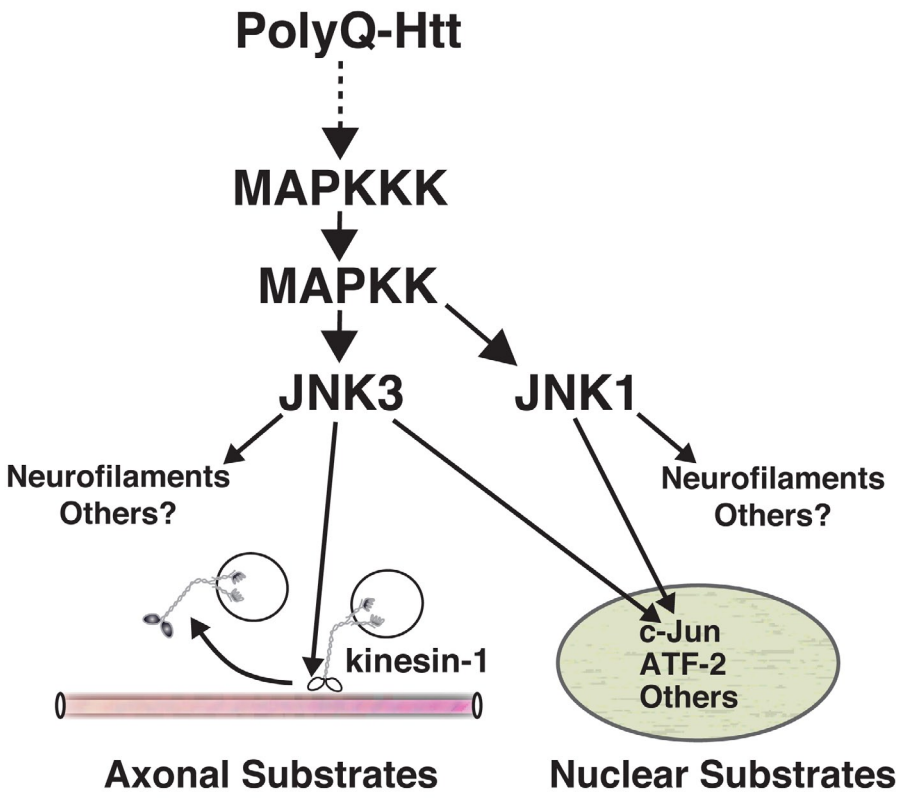


**Supplemental Figure 6. Inhibition of conventional kinesin-based motility induced by pathogenic Htt (polyQ-Htt).** Our results showing increased activation and phosphorylation of JNKs induced by polyQ-Htt suggest that this mutant polypeptide activates specific MAPKKKs and MAPKKs (dashed arrow) upstream of JNK. Increased JNK1 activation is linked to alterations in the activity of various transcription factors (i.e., ATF-2 and c-Jun, among others), consistent with widely reported changes in gene transcription in Huntington's disease[49]. Activation of JNK3 on the other hand, would lead to phosphorylation of kinesin-1 and likely other axonal substrates (question mark). Data in this work indicates that phosphorylation of kinesin-1s by JNK3 results in reduced binding of conventional kinesin to microtubules. Reductions in the delivery of critical axonal cargoes by conventional kinesin would result in impaired synaptic function and dying-back degeneration of neurons[3].

Nature Neuroscience: doi:10.1038/nn.2346

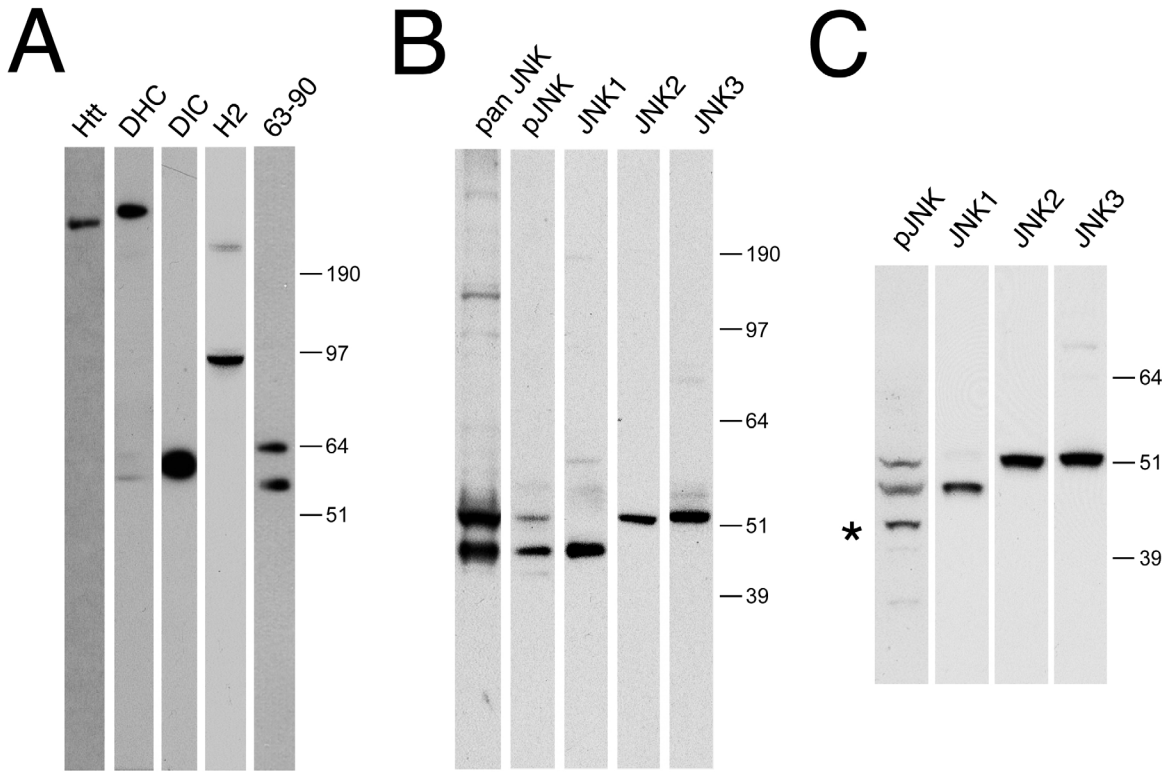


**Supplemental Figure 7: Characterization of antibodies used in this study. A)** Immunoblot analysis of whole mouse brain lysates using antibodies against molecular motors. From left to right: HTT: anti-huntingtin (2166, Chemicon); DHC), anti-dynein heavy chain (Santa Cruz #9115); DIC: anti-dynein intermediate chain (clone 74.1, Santa Cruz #13524); H2: anti-kinesin heavy chain (H2 clone, Chemicon)[13]; 63-90: anti-pan KLCs (63-90 clone, Chemicon)[13]. **B)** Immunoblot analysis of mouse striatum lysates using antibodies against JNKs. Pan-JNK: anti-pan-JNK (Upstate #06-748); pJNK: anti-phospho JNK (Cell Signaling #9251); JNK1: anti-JNK1 (Pharmingen #554268); JNK2: anti-JNK2 (Cell Signaling #4672); JNK3: anti-JNK3 (Cell Signaling #2305). **C)** Immunoblot analysis of NSC34 lysates using antibodies against JNKs. Antibodies are the same as in **B**. Molecular weight markers (Invitrogen#LC5925) are indicated at the left side of each panel. See Material and methods for a detailed description of SDS-PAGE conditions.